ACS OMEGA

http://pubs.acs.org/journal/acsodf

Article

Catalytic Enhancement of Cyclohexene Hydration by Ga-Doped ZSM-5 Zeolites

Yuzhen Jin, Lukuan Zong, Xiangyu Wang, and Huijuan Wei*

Cite This: *ACS Omega* 2022, 7, 26289−26297

Read Online

ACCESS | Metrics & More | Article Recommendations

ABSTRACT: Ga-doped ZSM-5 zeolites were directly synthesized by a facile one-step hydrothermal method without organic templates and calcination and then investigated in the cyclohexene hydration reaction. The structure, component, textural properties, and acidity of the as-prepared samples were examined by X-ray diffraction (XRD), scanning electron microscopy (SEM), X-ray fluorescence (XRF), Brunauer−Emmett−Teller (BET), ammonia temperature-programmed desorption (NH_3-TPD), pyridine-chemisorbed IR (Py-IR), and ^{71}Ga, ^{27}Al, ^{29}Si, and ^{1}H magic-angle spinning (MAS) NMR techniques. The characterization results showed that the introduction of Ga atoms into the ZSM-5 zeolite framework is much easier than Al atoms and beneficial to promote the formation of small-sized crystals. The number of Brønsted acid sites of Ga-doped ZSM-5 samples obviously increased compared with Ga0-ZSM-5. Additionally, the highest cyclohexanol yield (10.1%) was achieved over the Ga3-ZSM-5 sample, while the cyclohexanol yield of the Ga0-ZSM-5 sample was 8.6%. This result indicated that the improved catalytic performance is related to its larger external surface area, smaller particle size, and more Brønsted acid sites derived from Si−OH−Al and Si−OH−Ga of Ga3-ZSM-5. Notably, the green route reduces harmful gas emission and provides a basis for doping other heteroatoms to regulate the catalytic performance of zeolites, especially in industrial production.

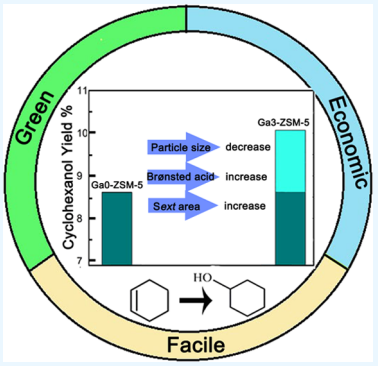

1. INTRODUCTION

Cyclohexanol is an important intermediate in the production of adipic acid and ε-caprolactam usually used in nylons, detergents, plasticizers, food additives, and pesticides production industry. Generally, its production processes are based on the oxidation of cyclohexane, hydrogenation of phenol, and direct hydration of cyclohexene.[1,2] Compared with the first two production routes, the direct hydration of the cyclohexene route has been widely used in the industrial production of cyclohexanol due to its high selectivity, safe operation, and energy saving.[3,4] ZSM-5 zeolites were used as a typical solid acid catalyst for the hydration reaction. However, the slow reaction rate and fairly low equilibrium conversion constrained the further development of this reaction although ZSM-5 catalysts are easily separated from the products and do not corrode equipment compared with liquid acid catalysts[5] Therefore, various modification methods on the ZSM-5 zeolite's structure and properties have been attempted to improve its catalytic performance in the cyclohexene hydration.[6−9] It is well accepted that ZSM-5 zeolites as a solid acid catalyst can provide enough protons for cyclohexene hydration reaction, which is considered to be an electrophilic addition reaction. Thus, the Brønsted acid sites in ZSM-5 zeolites are essential for understanding their catalytic performance in the hydration reaction.[10]

The acidic properties of ZSM-5 zeolites are related to the presence of protons compensating the negative charge generated by the trivalent Al atom substituting Si atoms in tetrahedral sites (T-sites). The resulting acidic bridging hydroxyl (Si−(OH)−Al) sites, also known as Brønsted acid sites, have opened zeolites as solid acid catalysts in the ketalization of glycerol with acetone, aromatization of methanol, oligomerization of propene, and methanol-to-olefins and cyclohexene hydration reactions.[11−15] The acidity of ZSM-5 zeolites is considered to provide active sites to tailor conversion and selectivity in a given reaction. Surprisingly, isomorphous substitution of Al atoms in tectosilicate frameworks is not the only pathway to improve the catalytic properties of zeolites. In the past decades, significant efforts have been made to obtain heteroatomic zeolites by isomorphic substitution of Si atoms in their parent structures by other elements such as Sn, B, Fe, Zr, Ge, Ga, or Ti. The resulting materials contain additional active sites influenced by the incorporation of T atoms and thus have many new applications.[16−22] Fang et al. prepared Ga-doped ZSM-5 zeolites via the isomorphic substitution method. The obtained

Received: April 2, 2022
Accepted: July 4, 2022
Published: July 19, 2022

sample exhibits a higher aromatic yield and better stability due to the $[GaO^+]^a$ species generating weaker Brønsted acid sites.[23] Bi et al. prepared a series of zeolites (ZSM-5, Ga-S1, MesoZSM-5, MesoGa-S1, and GaMesoZSM-5) based on tetrapropylammonium hydroxide (TPAOH) and [3-(trimethoxysilyl) propyl] octadecyldi-methylammonium chloride (TPOAC) as micropore and mesopore structure-directing agents respectively. GaMesoZSM-5 showed the highest yield of aromatics and effective reduction of phenols.[24] Ga-substituted zeolites were prepared using TPAOH as structure-directing agent by Xin et al. and displayed the highest benzene, toluene, ethylbenzene, and xylene selectivites in the aromatization reaction of *n*-heptane.[25]

According to the reviewed literature, an enhanced catalytic performance has been obtained on Ga-doped ZSM-5 zeolites. However, these synthesis approaches often bring about issues such as the production of harmful gases in the calcination process and additional post-treatment cost due to the use of expensive organic structure-directing agents.[26−28] Thus, it is of great research significance to improve the catalytic performance of ZSM-5 zeolites in cyclohexene hydration reaction by doping Ga by a green synthesis method.

Herein, a green and economical method was successfully developed for preparing Ga-doped ZSM-5 zeolites without an organic template using in situ seed-assistance method. The catalytic performance of as-prepared catalysts was evaluated in the cyclohexene hydration reaction. Furthermore, all of the samples obtained in this paper have not been calcined. Compared with the conventional methods, the process opens a green pathway to prepare zeolites with low energy consumption for commercialization.

2. EXPERIMENTAL SECTION

2.1. Synthesis of the Seed Suspension. Colloidal silica was purchased from Zhejiang Yuda Chemical Co., Ltd. Tetraethyl orthosilicate (TEOS), TPAOH (25 wt %), gallium nitrate hydrate ($Ga(NO_3)_3$), nitric acid (HNO_3), aluminum hydroxide ($Al(OH)_3$), and sodium hydroxide (NaOH) were bought from Sinopharm Chemical Reagent Co., Ltd.

Silicalite-1 (S-1) was used as seed for the ZSM-5 zeolites. It was synthesized by a previously reported procedure.[29,30] TEOS was added into TPAOH aqueous solution. The molar composition of the precursors was TEOS/0.2 TPAOH/20 H_2O. The mixture was stirred at room temperature for 2 h and then aged at 318 K for 24 h. Subsequently, the as-resulted solution was subject to hydrothermal treatment at 443 K for 24 h. The obtained S-1 suspension was directly employed as the seed.

2.2. Synthesis of ZSM-5 and Ga-Doped ZSM-5 Zeolites. Ga-doped ZSM-5 zeolites were synthesized by an in situ seed-assistance method. Specifically, colloidal silica (30 wt %) and $Ga(NO_3)_3$ (as silicon and gallium source) were mixed with distilled water to form solution A. Specified amounts of $Al(OH)_3$ and NaOH (as the alumina and alkali source) were first dissolved in distilled water, and the resultant solution was heated several minutes until the mixture became transparent (labeled as solution B). After that, the synthesis gel was prepared by mixing solutions A and B slowly under strenuous stirring. A homogeneous gel could be obtained after vigorous stirring for a period. Finally, 2.5 wt % self-made S-1 seed was added to the mixture, the molar composition of the mother gel is 12 Na_2O/100 SiO_2/3 Al_2O_3/*x* Ga_2O_3/2900 H_2O, and the Ga_2O_3 was added according to the different weight percentages of SiO_2. The gel was crystallized at 443 K for 36 h after aging at ambient temperature for 24 h. After predetermined crystallization periods, the autoclave was cooled and the synthesized solid product was recovered by centrifugation, washed with distilled water several times, and dried at 373 K for 12 h. The resulting solid product was labeled Ga*x*-ZSM-5 zeolites (*x* = 1, 2, 3, 4, 5). Ga0-ZSM-5 zeolites were synthesized according to the same preparation route as Ga*x*-ZSM-5 samples, except that the synthesis gel did not add Ga precursor.

In addition, the obtained Na-ZSM-5 zeolites were turned into H-form by conventional ion exchange with HNO_3 solution (1.0 mol·L^{-1}) at 313 K for 3 h with a liquid/solid ratio of 11 $cm^3 \cdot g^{-1}$. After that, the sample was centrifuged, washed, and dried at 373 K. All samples were dried using a conventional oven without calcination.

2.3. Characterization. Powder X-ray diffraction (XRD) analyses were recorded on a Panalytical X'Pert PRO diffraction meter (40 kV, 40 mA) using Cu Kα radiation source (λ = 1.540598 Å) at a scanning step of 1.2°·min^{-1} in the 2θ range of 5−50°. The relative crystallinity (RC) data of the samples were calculated by comparing the diffraction intensities of the five major peaks at 2θ = 7.8, 8.8, 23.0, 23.9, and 24.4°. Ga0-ZSM-5 was taken as a reference with 100%. The cell parameter of the samples was recorded via Unit Cell software. The textural properties of the zeolites were evaluated from the N_2 adsorption−desorption isotherms measured at 77 K using a Micromeritics ASAP2420 analyzer. Prior to N_2 adsorption, all of the samples were evacuated under vacuum for 12 h at 573 K. The Brunauer−Emmett−Teller (BET) method was employed to calculate the total surface area (S_{BET}) of the zeolites. The total pore volume (V_{tot}) was determined by a single-point method with the capillary condensation model from the volume adsorbed at P/P_0 = 0.99. The *t*-plot method was applied to calculate the micropore surface area (S_{mic}), external surface area (S_{ext}), and micropore volume (V_{mic}). The pore size distribution was calculated employing an adsorption branch of the isotherm according to the BJH (Barrett−Joyner−Halenda) method. Scanning electron micrographs (SEM) were taken on a Quanta FEG 250 scanning electron microscope to investigate the morphology of the prepared zeolites, and the agglomerate sizes of the samples were recorded from the micrographs using Nano Measurer 1.2 software. The elementary composition was measured by a PANalytical Axios-3600 X-ray fluorescence (XRF) spectrometer. ^{71}Ga, ^{27}Al, ^{29}Si, and ^{1}H magic-angle spinning (MAS) NMR experiments were performed on a Bruker Avance 400 spectrometer. The framework $(Si/Me)_{FW}$ ratio (Me = Al and Ga) was calculated using the following equation: $(Si/Me)_{FW}$ = (the total intensity of all of the ^{29}Si NMR signals)/(0.25 × the sum of $(MeO)Si(OSi)_3$), where Me is Al and Ga.[31,32] To evaluate the strength and amount of the acid sites of samples, the ammonia temperature-programmed desorption (NH_3-TPD) was performed on a Zhejiang Fantai Corp detector. Prior to the adsorption of ammonia, the catalyst was pretreated at 600 °C for 2 h in a flow of helium (1.0 mL·s^{-1}). Then, ammonia was adsorbed at 100 °C until saturated while a flow of helium was fed to remove the excess ammonia. The desorption of ammonia was carried out using a heating ramp of 10 °C·min^{-1} from 100 to 600 °C. Pyridine-chemisorbed IR (Py-IR) analysis was performed to determine the acid type of samples and recorded on a Thermo Nicolet IR 2000 spectrometer. According to the reported literature, the

https://doi.org/10.1021/acsomega.2c02031
ACS Omega 2022, 7, 26289−26297

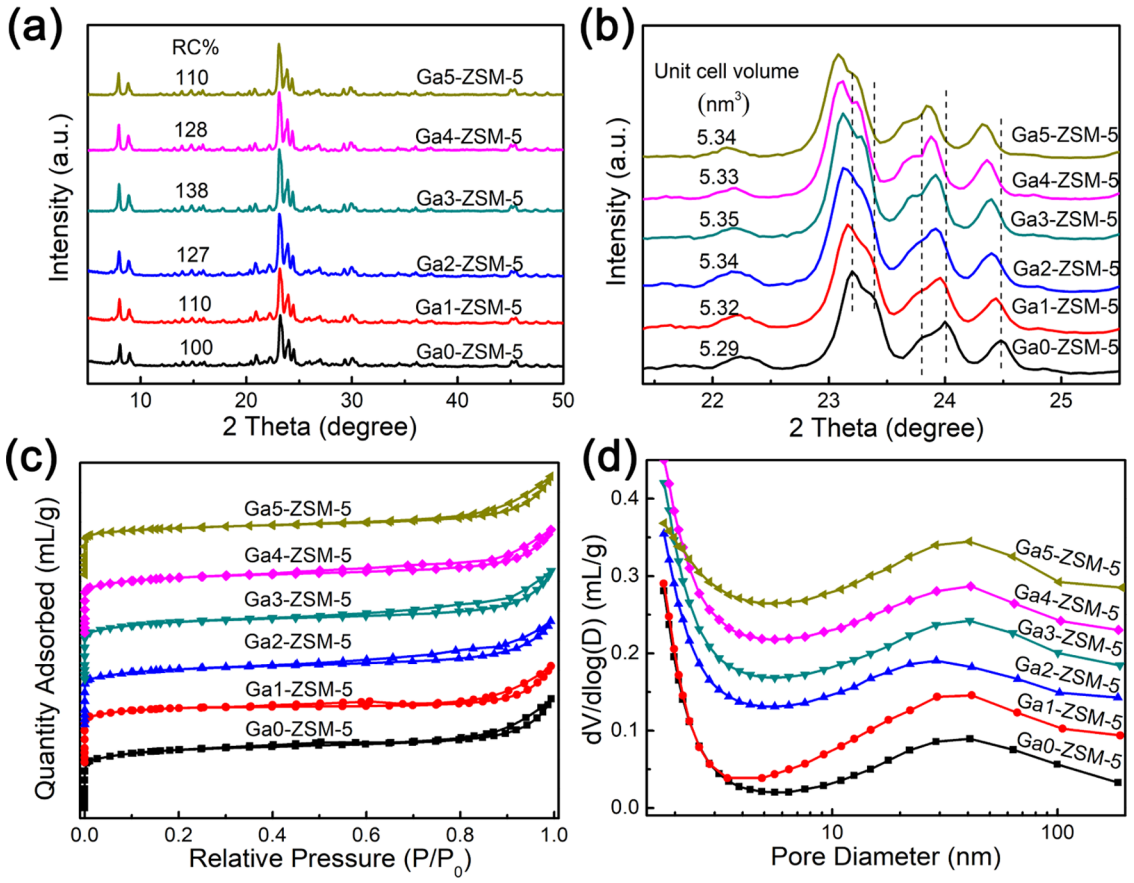

Figure 1. (a, b) XRD patterns, (c) N_2 adsorption−desorption isotherms, and (d) pore size distribution of ZSM-5 doped with different Ga contents.

amount of Bronsted and Lewis acid sites in samples was calculated.

2.4. Catalytic Evaluation: Cyclohexene Hydration Reaction. The catalytic performance of prepared samples for cyclohexene hydration was investigated in a 500 mL stainless-steel reactor equipped with agitation and temperature control instrument. For a typical run, 13.5 g of catalyst, 135 mL of water, and 135 mL of cyclohexene as reactants were first charged into the reactor. After being sealed up, the reactor was purged three times with nitrogen at a pressure of 0.15 MPa to evacuate the air. Subsequently, nitrogen was injected at 0.45 MPa initial pressure to ensure the reactants are liquid under the desired temperature. Thereafter, the temperature of the mixture was increased to 399 K and the reactor pressure was 0.6 MPa, and a slow stirring rate of 600 rpm was set to obtain uniform temperature distribution and avoid the deposition of catalysts. As the mixture was heated to the reaction temperature, an agitation speed of 900 rpm was set at the same time and the corresponding time was regarded as the initial time. Finally, the reactor was cooled in ice water to terminate the reaction after a fixed reaction time. After the reactor was kept static for several hours, it slowly depressurized to atmospheric pressure. The obtained samples from the organic phase were collected in a glass container and analyzed on a GC 9790 gas chromatograph equipped with an OV-1701 capillary column (30 m × 0.32 mm × 0.25 μm), using the internal standard analysis method. Furthermore, the yield (yield %) of cyclohexanol was calculated by the following equation

$$\text{yield}\ (\%) = n/n_0 \times 100\%$$

where n_0 is the initial mole of the cyclohexene. The n is the final mole of the cyclohexanol after reaction.

3. RESULTS AND DISCUSSION

3.1. Characterization of Ga-Doped ZSM-5. Figure 1a,b gives the XRD patterns of ZSM-5 zeolites doped with different Ga contents. All of Ga-doped samples possess characteristic peaks of MFI-type zeolites in the 2θ ranges of 7−9 and 22−25°, and the result implied that the topological structure of ZSM-5 zeolites was not damaged by doping Ga species. The finger peaks at 22.0−25.0° shifted toward lower diffraction angles because the Ga−O bond length (0.186 nm) is longer than the Al−O bond length (0.175 nm) and the Si−O bond length (0.164 nm), so the lattice spacing increase with the increase of Ga content. The result suggested that Ga species were introduced into the framework of ZSM-5 zeolites.[23,33,34] The cell volume of Ga-substituted ZSM-5 also increased compared with that of Ga0-ZSM-5, which further indicated that Ga atoms enter the lattice and become skeleton atoms. The relative crystallinity degrees of the Ga*x*-ZSM-5 samples are 100, 110, 127, 138, 128, and 110%. This is because the appropriate amount of Ga species is conducive to the formation of the lattice structure of ZSM-5, but excessive Ga may reduce the relative crystallinity of the sample due to the failure of bonding, which is consistent with the results reported by Han et al.[33] In addition, for all of the Ga*x*-ZSM-5 samples, no obvious crystal diffraction peak of Ga_2O_3 was observed.

https://doi.org/10.1021/acsomega.2c02031
ACS Omega 2022, 7, 26289−26297

Table 1. Chemical Composition of the Doped ZSM-5 Zeolites with Different Ga Contents

	gel composition		bulk composition			
sample	SiO_2/Al_2O_3	Ga_2O_3/SiO_2 (wt %)	SiO_2/Al_2O_3[a]	SiO_2/Al_2O_3[b]	Ga_2O_3/SiO_2 (wt %)[b]	Si/Me_{FW}[c]
Ga0-ZSM-5	33		28	27		13.9
Ga1-ZSM-5	33	3.05	30	28	0.33	13.3
Ga2-ZSM-5	33	4.41	29	28	0.48	
Ga3-ZSM-5	33	6.01	29	28	0.63	12.6
Ga4-ZSM-5	33	7.40	29	29	1.00	
Ga5-ZSM-5	33	10.27	30	29	1.28	10.9

[a]Measured by EDS. [b]Measured by XRF. [c]Si/Me_{FW} corresponds to the framework Si/(Al + Ga) ratio calculated by ^{29}Si MAS NMR.

The chemical compositions were analyzed by XRF and energy-dispersive X-ray spectroscopy (EDS), as shown in Table 1. The bulk SiO_2/Al_2O_3 molar ratio of Ga-doped ZSM-5 samples increased slightly as the Ga content increased, which indicated that the part of Al was more difficult to enter the bulk phase due to Ga incorporation via the isomorphous substitution method. It was also observed that the Ga_2O_3/SiO_2 (wt %) in the synthesized samples was only 10% of those in the corresponding initial gel, which implied that an appropriate amount of Ga can be introduced in the template-free synthesis system for ZSM-5 using inorganic material.

According to IUPAC, adsorption−desorption isotherms of all of the samples belong to type IV curves (Figure 1c). All samples display strong uptake at a low relative pressure, showing that all of the samples contain microporous structure. The small hysteresis loops at higher relative pressures could be ascribed to the interparticle voids between the smaller particles. As presented in Figure 1d, all samples exhibit a remarkable mesopore size distribution in the range of 10−90 nm. The textural properties of these samples are summarized in Table 2. The results indicated that the BET surface area, total pore volume, micropore area, and volume of the Ga-doped ZSM-5 zeolites decreased significantly with the increase of Ga content. Among them, Ga3-ZSM-5 shows larger external surface area and mesopore volume than those of the other samples, which is helpful to promote access to the active site for reactants and the diffusion of the products.

Table 2. Textural Properties of the Doped ZSM-5 Zeolites with Different Ga Contents

	surface area ($m^2 \cdot g^{-1}$)			pore volume ($cm^3 \cdot g^{-1}$)		
sample	S_{BET}	S_{mic}	S_{ext}	V_{total}	V_{mic}	V_{meso}
Ga0-ZSM-5	389	274	115	0.296	0.113	0.183
Ga1-ZSM-5	360	284	76	0.263	0.120	0.143
Ga2-ZSM-5	356	237	119	0.281	0.103	0.178
Ga3-ZSM-5	370	245	125	0.295	0.107	0.188
Ga4-ZSM-5	356	236	120	0.281	0.103	0.178
Ga5-ZSM-5	315	230	84	0.268	0.096	0.172

^{71}Ga, ^{27}Al, ^{29}Si, and ^{1}H MAS NMR measurements were performed. Figure 2a shows the ^{71}Ga MAS NMR spectra of Ga1-ZSM-5, Ga3-ZSM-5, and Ga5-ZSM-5 samples. The peak assigned to the tetrahedral framework Ga species at ca. 157 ppm is obviously observed for all of the Ga-doped zeolites, indicating that Ga species were successfully incorporated into the framework of the ZSM-5 zeolites synthesized using an in situ seed-assistance method.[35] A quantitative estimation of the content of framework Ga species through the integral area was performed. The sequence of Ga content in the obtained samples is Ga5-ZSM-5 (11.5×10^9) > Ga3-ZSM-5 (11.1×10^9) > Ga1-ZSM-5 (10.5×10^9). Moreover, the lack of signal at ca. 58 ppm implies that no extra-framework amorphous Ga_2O_3 particles are present in the Ga-doped ZSM-5 samples.[23]

Figure 2b displays the ^{27}Al MAS NMR spectra of Ga0-ZSM-5, Ga1-ZSM-5, Ga3-ZSM-5, and Ga5-ZSM-5 samples. The major signal at ca. 56 ppm is attributed to the four-coordinate Al species in the framework (FAl), while the peak at ca.1 ppm is categorized as the six-coordinate extra-framework Al (EFAl).[36] With increasing Ga content, the integral area of the FAl peak slightly decreases, demonstrating that the framework Al slightly decreases due to more Ga incorporation. ^{29}Si MAS NMR spectra of Ga0-ZSM-5, Ga1-ZSM-5, Ga3-ZSM-5, and Ga5-ZSM-5 samples are presented in Figure 2c. The signals ca. −105 and −112 ppm are corresponding to the $(MeO)Si(OSi)_3$ and $Si(OSi)_4$ sites in the framework structure, respectively.[33,34] The $(Si/Me)_{FW}$ ratio (Me = Al and Ga) was calculated from the ^{29}Si MAS NMR results and is listed in Table 1. The $(Si/Me)_{FW}$ ratio decreased with increasing Ga species in the bulk composition, while the Si/Al ratio slightly increased. This result indicates that Ga entered the skeleton of ZSM-5 zeolites more easily than Al. Therefore, it provides the possibility to form much more Brønsted acid sites.[37]

To evaluate the acid type (Brønsted and Lewis), strength, and content of the Ga0-ZSM-5 and Ga-doped ZSM-5 zeolites (H^+ form), all samples ion-exchanged directly with the HNO_3 solution without precalcining were performed by NH_3-TPD (Figure 2e), ^{1}H MAS NMR (Figure 2d), and Py-IR technology (Figure 2f). The NH_3-TPD analysis results are depicted in Figure 2e. All of the profiles of the samples display two obvious NH_3 desorption peaks located at temperatures ranging from 150 and 260 and from 400 to 500 °C. The peak at the lower temperature was assigned to the ammonia species either adsorbed (weakly chemisorbed) and/or held in place by means of hydrogen bridging bonds (physisorbed), whereas the other desorption peak at a higher temperature is related to the ammonia desorption on the strong acid sites (such as framework-coordinated aluminum or gallium sites).[38−42] The calculated acid amount based on NH_3-TPD is shown in Table 3. It can be seen the weak acid amount shows a decreasing trend and the strong acid amount increases after Ga was doped into ZSM-5 zeolites. Solid-state ^{1}H MAS NMR was used to study the Brønsted acid sites in solid acid catalysts.[43,44] As shown in Figure 2d, the signal at 6.3 ppm corresponds to bridging OH groups derived from Si−O(H)−Al and the signal at 1.9 ppm is assigned to Si−OH groups at framework defects.[45] Compared with the Ga0-ZSM-5 sample, an additional peak at 4.5 ppm due to bridging OH groups and produced Si−O(H)−Ga groups appears on the Ga-doped ZSM-5 zeolites.[46] Therefore, the Brønsted acid of Ga-doped ZSM-5 zeolites is derived from Si−OH−Me (Ga and Al).

https://doi.org/10.1021/acsomega.2c02031
ACS Omega 2022, 7, 26289−26297

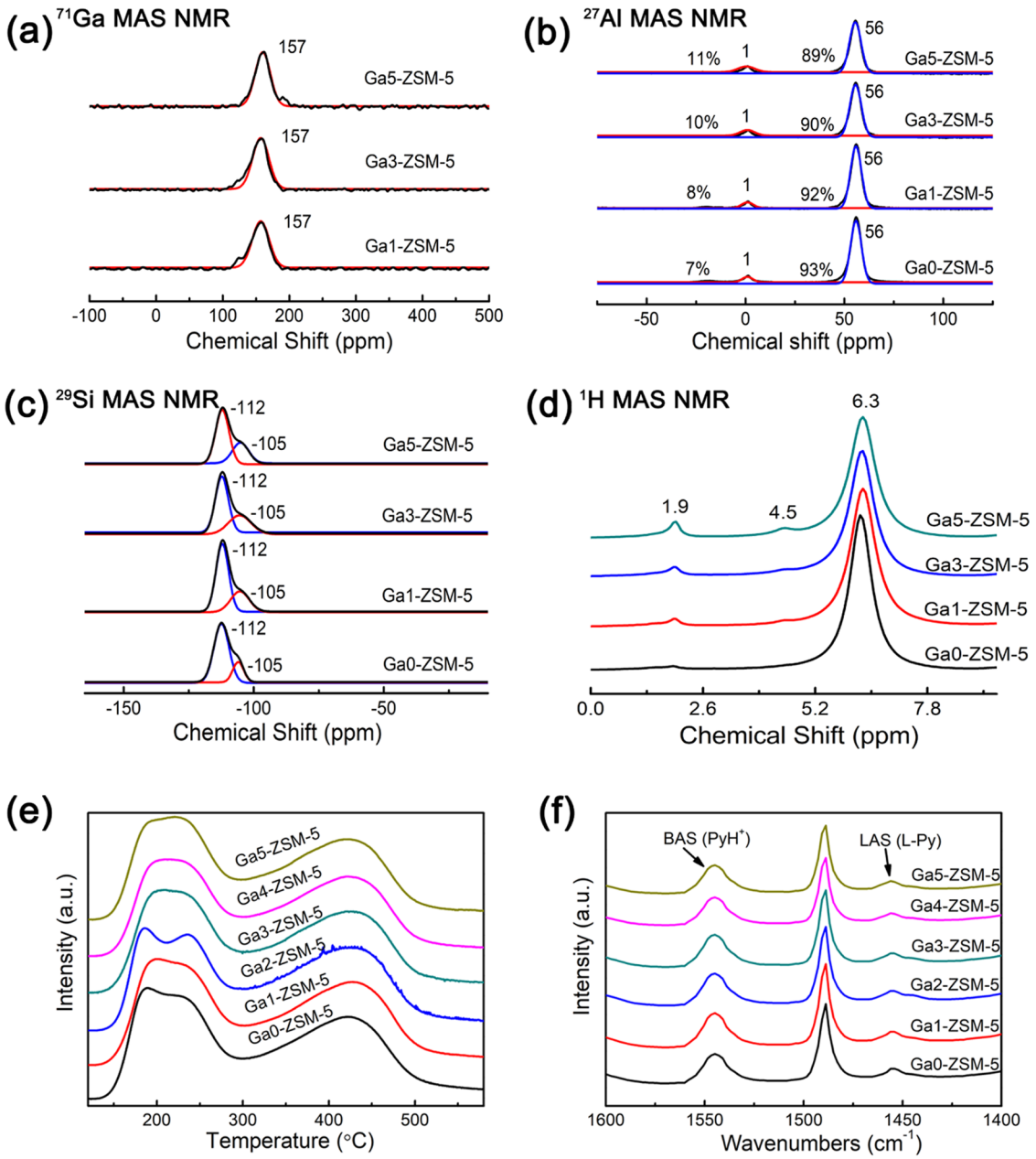

Figure 2. (a) ^{71}Ga MAS NMR spectra, (b) ^{27}Al MAS NMR spectra, (c) ^{29}Si MAS NMR spectra, (d) ^{1}H MAS NMR spectra, (e) NH_3-TPD profiles, and (f) pyridine-IR spectra of ZSM-5 zeolites doped with different Ga contents.

Table 3. Acid Property of Doped ZSM-5 Zeolites with Different Ga Contents

	distribution of acid sites (mmol·g^{-1})			acidity (mmol·g^{-1})	
sample	weak acid	strong acid	total	Brønsted	Lewis
Ga0-ZSM-5	0.45	0.50	0.95	0.41	0.07
Ga1-ZSM-5	0.39	0.55	0.94	0.45	0.07
Ga2-ZSM-5	0.38	0.54	0.92	0.47	0.09
Ga3-ZSM-5	0.38	0.56	0.94	0.50	0.08
Ga4-ZSM-5	0.38	0.53	0.91	0.52	0.08
Ga5-ZSM-5	0.41	0.54	0.96	0.53	0.09

Pyridine-IR was also performed to further provide detailed information on both Brønsted and Lewis acid sites. The Py-IR results in Figure 2f showed that the band at about 1545 cm^{-1} stems from PyH^+ generated by the charge interaction of pyridine and H^+ (Brønsted acid sites), which was indicative of Brønsted acid. The band located at 1455 cm^{-1} is attributed to the coordination between pyridine and Lewis acid site originating from unsaturated coordinated Al or Ga ions, which is often used to characterize Lewis acid. The band about 1490 cm^{-1} is commonly assigned to the co-contribution of pyridine adsorbed over the Brønsted and Lewis acid site. It should be pointed out that the quantity of the Brønsted and Lewis acid both enhanced as the Ga content increased, especially the increase of Brønsted acid amount is much more obvious (Table 3). The Brønsted acid content of the Ga5-ZSM-5 zeolite increased to 0.53 mmol·g^{-1}, indicating that Ga doping in the synthetic system by seed-assistance method contributes to the formation of Brønsted acid sites in ZSM-5 zeolites.[23]

https://doi.org/10.1021/acsomega.2c02031
ACS Omega 2022, 7, 26289−26297

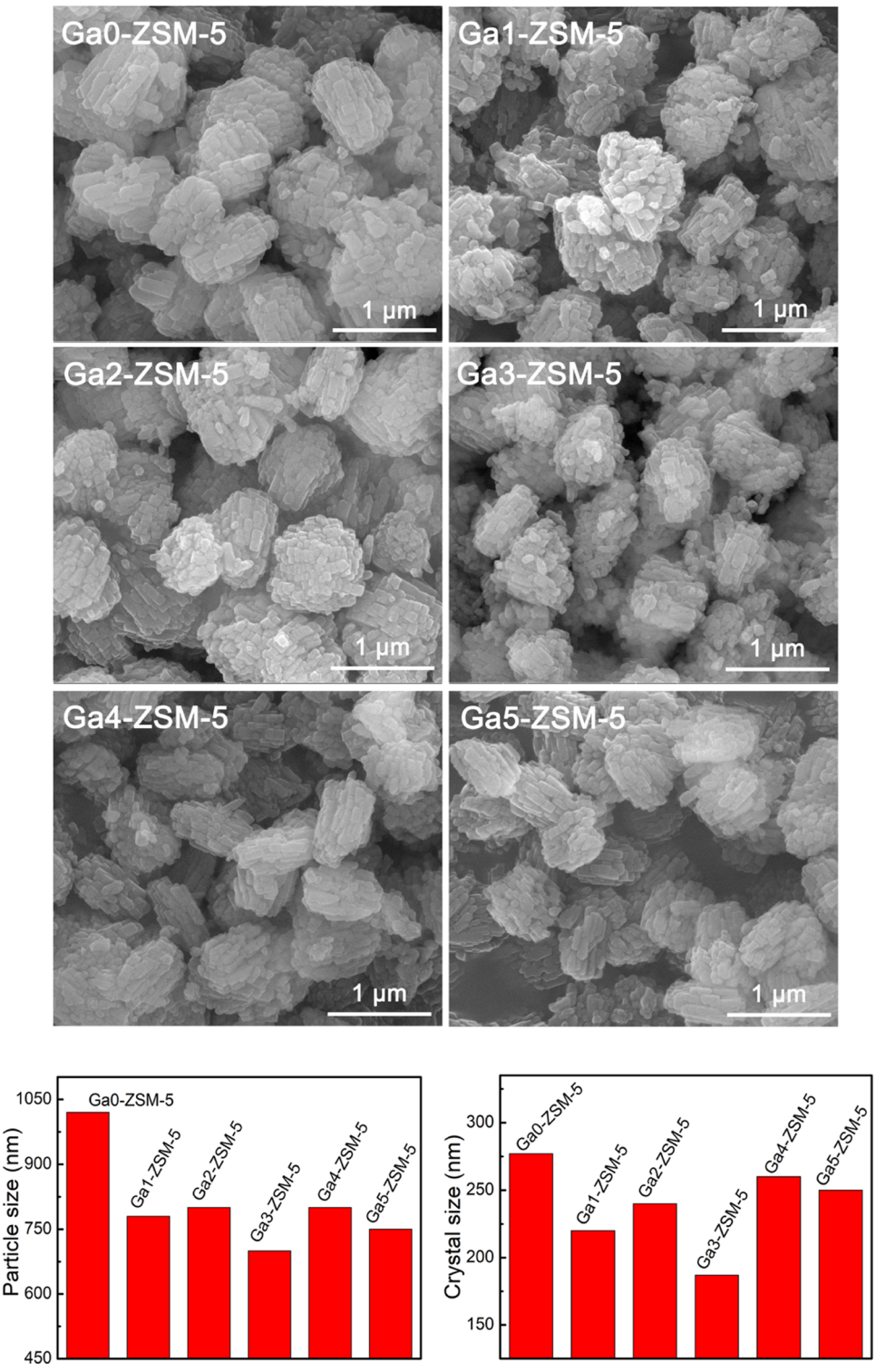

Figure 3. SEM images, particle size, and crystal size of ZSM-5 doped with different Ga contents.

SEM images of all of the Ga-doped ZSM-5 samples are shown in Figure 3. The particle of Ga0-ZSM-5 presented ellipsoidal aggregates with a size of about 1 μm, and the outer surface is composed of stacked nanocrystallites of about 277 nm. Ga-substituted ZSM-5 exhibited a similar aggregated morphology to Ga0-ZSM-5 but particle size and stacked nanocrystallites constructing the outer surface size both decreased. Ga in the synthetic system can effectively promote crystal nucleus formation and reduce nanocrystallite size. The result was in agreement with the phenomenon reported by Fang and Han et al.[33,23]

3.2. Catalytic Performance. The catalytic performances of the synthesized Ga0-ZSM-5 and Ga-doped ZSM-5 samples for cyclohexene hydration reaction are present in Figure 4. With the increase in Ga doping amount, the cyclohexanol yield of Ga-doped ZSM-5 samples increased first and then decreased. The cyclohexanol yields were 8.4 and 8.6% for commercialized ZSM-5 and Ga0-ZSM-5, respectively, but

https://doi.org/10.1021/acsomega.2c02031
ACS Omega 2022, 7, 26289−26297

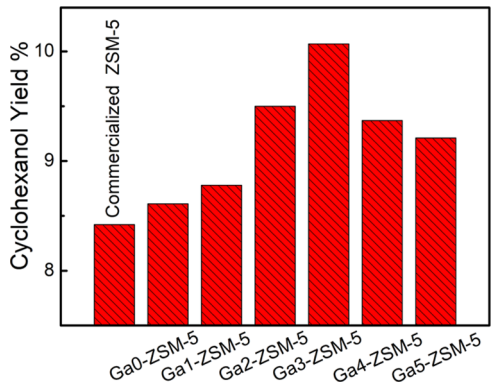

Figure 4. Catalytic performances of ZSM-5 zeolites with different Ga contents. Reaction time: 60 min, temperature: 126−128 °C, stirring speed: 900 rpm, pressure: 0.6−0.7 MPa.

Ga3-ZSM-5 exhibited superior catalytic results and the cyclohexanol yield was up to 10.1%. It has been acknowledged that cyclohexene hydration reaction is an electrophilic addition reaction and ZSM-5 zeolites are typical solid acid catalysts that can provide Brønsted acid for this reaction.[33] The classical mechanism is that the reaction proceeds by the carbenium ion route through cyclohexene adsorbed on the Brønsted acid sites. The other mechanism proposed that the water molecule is adsorbed on the catalyst to form a hydroxonium ion H_3O^+, which further reacts with the cyclohexene molecule to form cyclohexanol.[47] However, it is conceivable that the Brønsted acid sites are the active sites. After Ga was doped in the ZSM-5 zeolites, ^{29}Si MAS NMR results indicate that Ga entered the skeleton of ZSM-5 zeolites more easily than Al. It provides the possibility to form much more Brønsted acid sites. The amount of Brønsted acid enhanced obviously as the Ga content increased. Therefore, the catalytic performance of Ga-ZSM-5 zeolites was improved.

In addition, cyclohexene hydration is a three-phase reaction of water, oil, and solid catalyst. The physical structure of the catalysts, such as particle size and mesopore channels, also affects the diffusion process of the reactants to the catalytic active Brønsted acid site, thus affecting catalytic performance.[5,10,48] Therefore, the improvement of catalytic performance of Ga-doped ZSM-5 samples is related to the increase of Brønsted acid site content, but there is no linear relationship. The number of Brønsted acid sites in Ga3-ZSM-5 was lower than that in Ga4-ZSM-5 and Ga5-ZSM-5 samples, but its catalytic activity was superior. The reason is that the fine grains, larger surface area, and mesopore volume of Ga3-ZSM-5 contribute to the diffusion of reactants and product molecules. In general, in situ doping of an appropriate amount of Ga by the template-free method can improve the catalytic performance of the ZSM-5 sample for cyclohexene hydration.

4. CONCLUSIONS

In conclusion, a series of Ga-doped ZSM-5 zeolites with different Ga contents were successfully prepared for an in situ seed-assistance method and used for the cyclohexene hydration reaction. The physical characterizations of the synthesized samples were examined by XRD, SEM, BET, NH_3-TPD, XRF, Py-IR, ^{71}Ga, ^{27}Al, ^{29}Si, and ^{1}H MAS NMR. The obtained results indicated that Ga was incorporated into the ZSM-5 zeolites skeleton without changing the MFI structure. The particle size of Ga-doped ZSM-5 samples reduced remarkably owing to the crystal nuclei forming more easily compared with the Ga0-ZSM-5 sample. And the Brønsted acid sites content increased gradually with the introduction of Ga species. The Ga3-ZSM-5 sample displayed the best catalytic performance with the highest cyclohexanol yield. The reason can be ascribed to the synergistic effect of the shortened diffusion length and additional active sites. This green and economically favorable synthesis route is a promising pathway for the adjustment of acidity in zeolites.

AUTHOR INFORMATION

Corresponding Author

Huijuan Wei − *Green Catalysis Center, and College of Chemistry, Zhengzhou University, Zhengzhou 450001, P. R. China;* orcid.org/0000-0001-7108-5943; Email: weihuijuan@zzu.edu.cn

Authors

Yuzhen Jin − *Green Catalysis Center, and College of Chemistry, Zhengzhou University, Zhengzhou 450001, P. R. China*

Lukuan Zong − *Green Catalysis Center, and College of Chemistry, Zhengzhou University, Zhengzhou 450001, P. R. China; Zhejiang Medicine Co, Ltd., Changhai Biological Branch, Shaoxing 312000, P.R. China*

Xiangyu Wang − *Green Catalysis Center, and College of Chemistry, Zhengzhou University, Zhengzhou 450001, P. R. China*

Complete contact information is available at: https://pubs.acs.org/10.1021/acsomega.2c02031

Notes

The authors declare no competing financial interest.

ACKNOWLEDGMENTS

The authors gratefully acknowledge the financial support from the Science and Technology Project of Henan Province, China (grant 212102210216).

REFERENCES

(1) Estahbanati, M. R. K.; Feilizadeh, M.; Babin, A.; Mei, B.; Mul, G.; Iliuta, M. C. Selective photocatalytic oxidation of cyclohexanol to cyclohexanone: a spectroscopic and kinetic study. *Chem. Eng. J.* **2020**, *382*, No. 122732.

(2) Zhu, Y.; Gao, L.; Wen, L.; Zong, B.; Wang, H.; Qiao, M. Cyclohexene esterification-hydrogenation for efficient production of cyclohexanol. *Green Chem.* **2021**, *23*, 1185−1192.

(3) Liu, X.; Luo, H.; Lei, Y.; Wu, X.; Gani, R. Heat-pump-assisted reactive distillation for direct hydration of cyclohexene to cyclohexanol: a sustainable alternative. *Sep. Purif. Technol.* **2022**, *280*, No. 119808.

(4) Zheng, H.; Lin, M.; Qiu, T.; Shen, Y.; Tian, H.; Zhao, S. Simulation study of direct hydration of cyclohexene to cyclohexanol using isophorone as cosolvent. *Chem. Eng. Res. Des.* **2017**, *117*, 346−354.

(5) Hu, M.; Tian, H. Design of process and control scheme for cyclohexanol production from cyclohexene using reactive distillation. *Chin. J. Chem. Eng.* **2021**, *40*, 96−105.

(6) Wang, S.; Li, C.; Wen, Y.; Wei, H.; Li, B.; Wang, X. Microparticle HZSM-5 zeolite as highly active catalyst for the hydration of cyclohexene to cyclohexanol. *Res. Chem. Intermed.* **2016**, *42*, 8131−8142.

(7) Meng, F.; Wang, Y.; Wang, S.; Wang, S. Hydration of cyclohexene over zeolite ZSM-5: improved catalyst performance by alkali treatment. *React. Kinet., Mech. Catal.* **2016**, *119*, 671−683.

(8) Yufei, S.; Liu, Y.; Wei, H.; Wang, X. Effects of calcination temperature on catalytic performances of HZSM-5 zeolites in hydration of cyclohexene. *Petrochem. Technol.* **2013**, *42*, 1373−1377.
(9) Spod, H.; Lucas, M.; Claus, P. Hydration of cyclohexene into cyclohexanol using H-ZSM5 as catalyst. *Chem. Ing. Tech.* **2017**, *89*, 750−756.
(10) Treps, L.; Gomez, A.; de Bruin, T.; Chizallet, C. Environment, stability and acidity of external surface sites of Silicalite-1 and ZSM-5 micro and nano slabs, sheets, and crystals. *ACS Catal.* **2020**, *10*, 3297−3312.
(11) Huang, X.; Zhang, G.; Zhang, Lu.; Zhang, Q. Continuous flow synthesis of a ZSM-5 film in capillary microchannel for efficient production of solketal. *ACS Omega* **2020**, *5*, 20784−20791.
(12) Biligetu, T.; Wang, Y.; Nishitoba, T.; Otomo, R.; Park, S.; Mochizuki, H.; Kondo, J. N.; Tatsumi, T.; Yokoi, T. Al distribution and catalytic performance of ZSM-5 zeolites synthesized with various alcohols. *J. Catal.* **2017**, *353*, 1−10.
(13) Hawkins, A. P.; Zachariou, A.; Parker, S.; Collier, P.; Silverwood, I.; Howe, R.; Lennon, D. Onset of propene oligomerization reactivity in ZSM-5 studied by inelastic neutron scattering spectroscopy. *ACS Omega* **2020**, *5*, 7762−7770.
(14) Lai, P.-C.; Chen, C.; Hsu, H.; Lee, C.; Lin, Y. Methanol aromatization over Ga-doped desilicated HZSM-5. *RSC Adv.* **2016**, *6*, 67361.
(15) Chen, K.; Gan, Z.; Horstmeier, S.; White, J. Distribution of aluminum species in zeolite catalysts: Al-27 NMR of framework, partially-coordinated framework, and non-framework moieties. *J. Am. Chem. Soc.* **2021**, *143*, 6669−6680.
(16) Yang, X.; Wang, F.; Wei, R.; Li, S.; Wu, Y.; Shen, P.; Wang, H.; Gao, L.; Xiao, G. Synergy effect between hierarchical structured and Sn-modified H [Sn, Al] ZSM-5 zeolites on the catalysts for glycerol aromatization. *Microporous Mesoporous Mater.* **2018**, *257*, 154−161.
(17) Yaripour, F.; Shariatinia, Z.; Sahebdelfar, S.; Irandoukht, A. Effect of boron incorporation on the structure, products selectivities and lifetime of H-ZSM-5 nanocatalyst designed for application in methanol-to-olefins (MTO) reaction. *Microporous Mesoporous Mater.* **2015**, *203*, 41−53.
(18) Li, J.; Han, D.; He, T.; Liu, G.; Zi, Z.; Wang, Z.; Wu, J.; Wu, J. Nanocrystal H [Fe, Al] ZSM-5 zeolites with different silica-alumina composition for conversion of dimethyl ether to gasoline. *Fuel Process. Technol.* **2019**, *191*, 104−110.
(19) Kore, R.; Satpati, B.; Srivastava, R. Highly efficient and green chemical synthesis of imidazolyl alcohols and N-imidazolyl functionalized β-amino compounds using nanocrystalline ZSM-5 catalysts. *Appl. Catal., A* **2014**, *477*, 8−17.
(20) Lou, Y.; Marinkovic, S.; Estrine, B.; Qiang, W.; Enderlin, G. Oxidation of furfural and furan derivatives to maleic acid in the presence of a simple catalyst system based on acetic acid and TS-1 and hydrogen peroxide. *ACS Omega* **2020**, *5*, 2561−2568.
(21) Kore, R.; Srivastava, R.; Satpati, B. Highly efficient nanocrystalline zirconosilicate catalysts for the aminolysis, alcoholysis, and hydroamination reactions. *ACS Catal.* **2013**, *3*, 2891−2904.
(22) Xia, C.; Liu, Y.; Lin, M.; Peng, X.; Zhu, B.; Shu, X. Confirmation of the isomorphous substitution by Sn atoms in the framework positions of MFI-typed zeolite. *Catal. Today* **2018**, *316*, 193−198.
(23) Fang, Y.; Su, X.; Bai, X.; Wu, W.; Wang, G.; Xiao, L.; Yu, A. Aromatization over nanosized Ga-containing ZSM-5 zeolites prepared by different methods: Effect of acidity of active Ga species on the catalytic performance. *J. Energy Chem.* **2017**, *26*, 768−775.
(24) Bi, C.; Wang, X.; You, Q.; Liu, B.; Li, Z.; Zhang, J.; Hao, Q.; Sun, M.; Chen, H.; Ma, X. Catalytic upgrading of coal pyrolysis volatiles by Ga-substituted mesoporous ZSM-5. *Fuel* **2020**, *267*, No. 117217.
(25) Xin, M.; Xing, E.; Gao, X.; Wang, Y.; Ouyang, Y.; Xu, G.; Luo, Y.; Shu, X. Ga substitution during modification of ZSM-5 and its influences on catalytic aromatization performance. *Ind. Eng. Chem. Res.* **2019**, *58*, 6970−6981.
(26) Yue, Y.; Kang, Y.; Bai, Y.; Gu, L.; Liu, H.; Bao, J.; Wang, T.; Yuan, P.; Zhu, H.; Bai, Z.; Bao, X. Seed-assisted, template-free synthesis of ZSM-5 zeolite from natural aluminosilicate minerals. *Appl. Clay Sci.* **2018**, *158*, 177−185.
(27) Krishnamurthy, G.; Bhan, A.; Delgass, W. Identity and chemical function of gallium species inferred from microkinetic modeling studies of propane aromatization over Ga/HZSM-5 catalysts. *J. Catal.* **2010**, *271*, 370−385.
(28) Schreiber, M. W.; Plaisance, C.; Baumgärtl, M.; Reuter, K.; Jentys, A.; Bermejo-Deval, R.; Lercher, J. Lewis-Brønsted acid pairs in Ga/H-ZSM-5 to catalyze dehydrogenation of light alkanes. *J. Am. Chem. Soc.* **2018**, *140*, 4849−4859.
(29) Huang, M.; Wen, Y.; Wei, H.; Zong, L.; Gao, X.; Wu, K.; Wang, X.; Liu, M. The clean synthesis of small-particle TS-1 with high-content framework Ti by using NH_4HCO_3 and suspended seeds as an assistant. *ACS Omega* **2021**, *6*, 13015−13023.
(30) Liu, M.; Chang, Z.; Wei, H.; Li, B.; Wang, X.; Wen, Y. Low-cost synthesis of size-controlled TS-1 by using suspended seeds: From screening to scale-up. *Appl. Catal., A* **2016**, *525*, 59−67.
(31) Yu, Z.; Zheng, A.; Wang, Q.; Chen, L.; Xu, J.; Amoureux, J.; Deng, F. Insights into the dealumination of zeolite HY revealed by sensitivity-enhanced ^{27}Al DQ-MAS NMR spectroscopy at high field. *Angew. Chem., Int. Ed.* **2010**, *49*, 8657−8661.
(32) Wei, R.; Li, C.; Yang, C.; Shan, H. Effects of ammonium exchange and Si/Al ratio on the conversion of methanol to propylene over a novel and large partical size ZSM-5. *J. Nat. Gas Chem.* **2011**, *20*, 261−265.
(33) Han, Z.; Zhou, F.; Liu, Y.; Qiao, K.; Ma, H.; Yu, L.; Wu, G. Synthesis of gallium-containing ZSM-5 zeolites by the seed-induced method and catalytic performance of GaZSM-5 and AlZSM-5 during the conversion of methanol to olefins. *J. Taiwan Inst. Chem. Eng.* **2019**, *103*, 149−159.
(34) Jiang, X.; Su, X.; Bai, X.; Li, Y.; Yang, L.; Zhang, K.; Zhang, Y.; Liu, Y.; Wu, W. Conversion of methanol to light olefins over nanosized [Fe, Al] ZSM-5 zeolites: Influence of Fe incorporated into the framework on the acidity and catalytic performance. *Microporous Mesoporous Mater.* **2018**, *263*, 243−250.
(35) Gao, P.; Xu, J.; Qi, G.; Wang, C.; Wang, Q.; Zhao, Y.; Zhang, Y.; Feng, N.; Zhao, X.; Li, J.; Deng, F. A mechanistic study of methanol-to-aromatics reaction over Ga-modified ZSM-5 zeolites: understanding the dehydrogenation process. *ACS Catal.* **2018**, *8*, 9809−9820.
(36) Yang, Y.; Sun, C.; Du, J.; Yue, Y.; Hua, W.; Zhang, C.; Shen, W.; Xu, H. The synthesis of endurable B-Al-ZSM-5 catalysts with tunable acidity for methanol to propylene reaction. *Catal. Commun.* **2012**, *24*, 44−47.
(37) Losch, P.; Joshi, H.; Vozniuk, O.; Grünert, A.; Ochoa-Hernández, C.; Jabraoui, H.; Badawi, M.; Schmidt, W. Proton mobility, intrinsic acid strength, and acid site location in zeolites revealed by varying temperature infrared spectroscopy and density functional theory studies. *J. Am. Chem. Soc.* **2018**, *140*, 17790−17799.
(38) Jia, C.; Zong, L.; Wen, Y.; Xu, H.; Wei, H.; Wang, X. Synthesis and scale-up of ZSM-5 aggregates with hierarchical structure. *Res. Chem. Intermed.* **2019**, *45*, 3913−3927.
(39) Khallouk, K.; Solhy, A.; Idrissi, N.; Flaud, V.; Kherbeche, A.; Barakat, A. Microwave-assisted selective oxidation of sugars to carboxylic acids derivatives in water over zinc-vanadium mixed oxide. *Chem. Eng. J.* **2020**, *385*, No. 123914.
(40) Yang, N.-z.; Guo, R.; Pan, W.; Chen, Q.; Wang, Q.; Lu, C. The promotion effect of Sb on the Na resistance of Mn/TiO_2 catalyst for selective catalytic reduction of NO with NH_3. *Fuel* **2016**, *169*, 87−92.
(41) Ma, T.; Zhang, L.; Song, Y.; Shang, Y.; Zhai, Y.; Gong, Y. A comparative synthesis of ZSM-5 with ethanol and TPABr template: Distinction of Brönsted/Lewis acidity ratio and its impact on n-hexane cracking. *Catal. Sci. Technol.* **2018**, *8*, 1923−1935.
(42) Al-Dughaither, A. S.; de Lasa, H. HZSM-5 zeolites with different SiO_2/Al_2O_3 ratios. characterization and NH_3 desorption kinetics. *Ind. Eng. Chem. Res.* **2014**, *53*, 15303−15316.

https://doi.org/10.1021/acsomega.2c02031
ACS Omega 2022, 7, 26289−26297

(43) Chen, X.; Fu, Y. Y.; Yue, B.; He, H. Y. Acidity and Basicity of Solid Acid Catalysts Studied by Solid-State NMR. *Chin. J. Magn. Reson.* **2021**, *38*, 491−502.
(44) Peng, Y.-K.; Edman Tsang, S. Probe-assisted NMR: Recent progress on the surface study of crystalline metal oxides with various terminated facets. *Magn. Reson. Lett.* **2022**, *2*, 9−16.
(45) Gabrienko, A. A.; Danilova, I. G.; Arzumanov, S. S.; Pirutko, L. V.; Freude, D.; Stepanov, A. G. Direct measurement of zeolite Brønsted acidity by FTIR spectroscopy. solid-state H MAS NMR approach for reliable determination of the integrated molar absorption coefficients. *J. Phys. Chem. C* **2018**, *122*, 25386−25395.
(46) Zhang, L.; Yang, L.; Liu, R.; Shao, X.; Dai, W.; Wu, G. J.; Guan, N. J.; Guo, Z. H.; Zhu, W. P.; Li, L. D. Design of plate-like H[Ga]MFI zeolite catalysts for high-performance methanol-to-propylene reaction. *Microporous Mesoporous Mater.* **2022**, *333*, No. 111767.
(47) Shan, X.; Cheng, Z.; Yuan, P. Reaction kinetics and mechanism for hydration of cyclohexene over ion-exchange resin and H-ZSM-5. *Chem. Eng. J.* **2011**, *175*, 423−432.
(48) Kim, S.; Park, G.; Woo, M.; Kwak, G.; Kim, S. Control of hierarchical structure and framework-Al distribution of ZSM-5 via adjusting crystallization temperature and their effects on methanol conversion. *ACS Catal.* **2019**, *9*, 2880−2892.

https://doi.org/10.1021/acsomega.2c02031
ACS Omega 2022, 7, 26289−26297